## Supplemental Figure 1



**Supplemental Figure 1. Renin lineage cells contribute to arteriolar hypertrophy in a polyclonal way.** Kidney tissues from *Ren1cKO;Ren1c-Cre;Confetti* and control mice. Masson's Trichrome staining, immunohistochemistry for α-SMA showed the progression of the renal disease with aging. Frozen sections showed that the policlonality was maintained during the disease progression. Scale bars, 50 µm. α-SMA; alpha-smooth muscle actin, *Ren1cKO*; *Ren1c* gene knockout.

**Supplemental Figure 2. Transcriptome of *Renin^null* cells with the Fluidigm C1 system.** (**A**) The UMAP with all the cells after normalization. (**B**) Feature plots and ridge plots for *Ren1*, *Akr1b7*, and *YFP*. (**C**) ISH for *Ren1* and *Akr1b7* mRNA. *Akr1b7* positive cells were increased in kidneys from *Ren1^cKO* mice. Scale bars, 50 μm. (**D**) Ridge plots of smooth muscle genes (*Acta2, Mhy11, Tagln*, and *Cnn1*). ISH; *in situ* hybridization, *Ren1^cKO*; *Ren1^c* gene knockout, UMAP; Uniform Manifold Approximation and Projection, WT; wild-type.
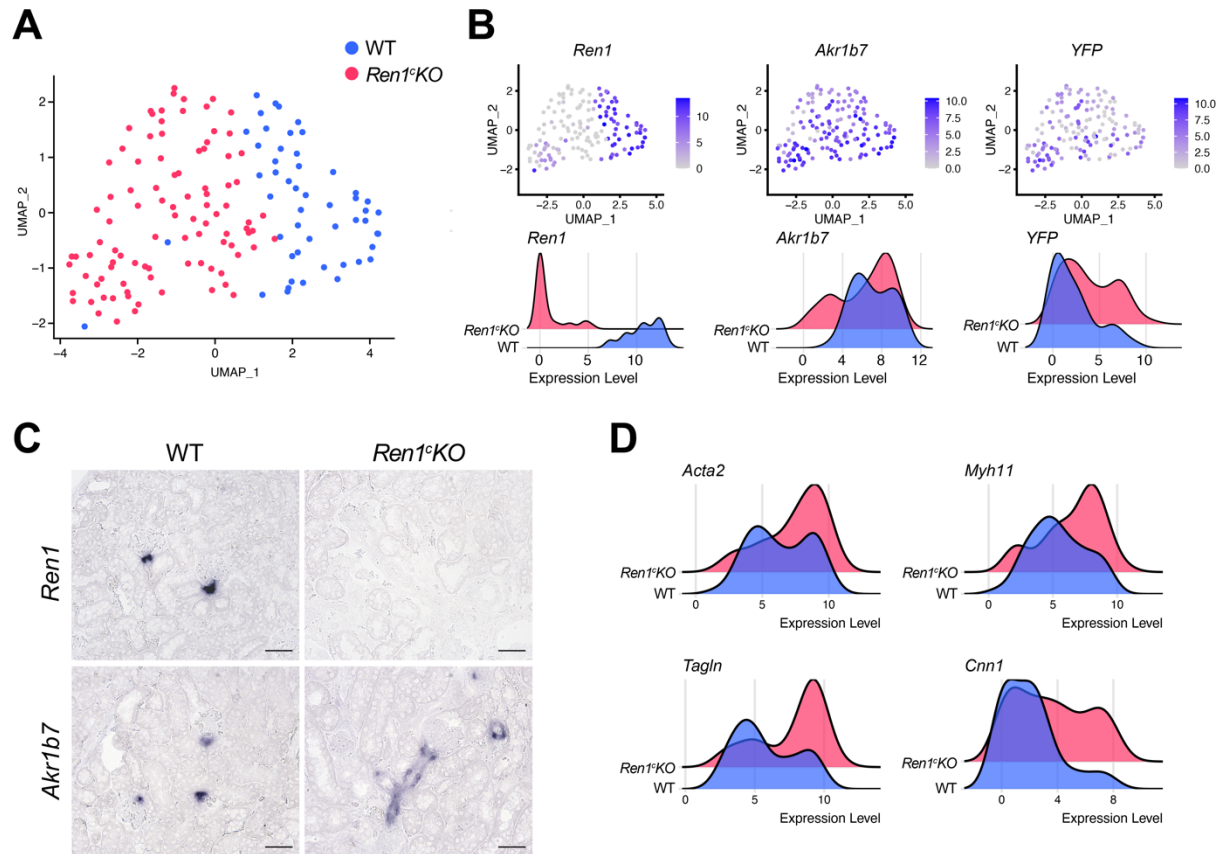
**Supplemental Figure 3**
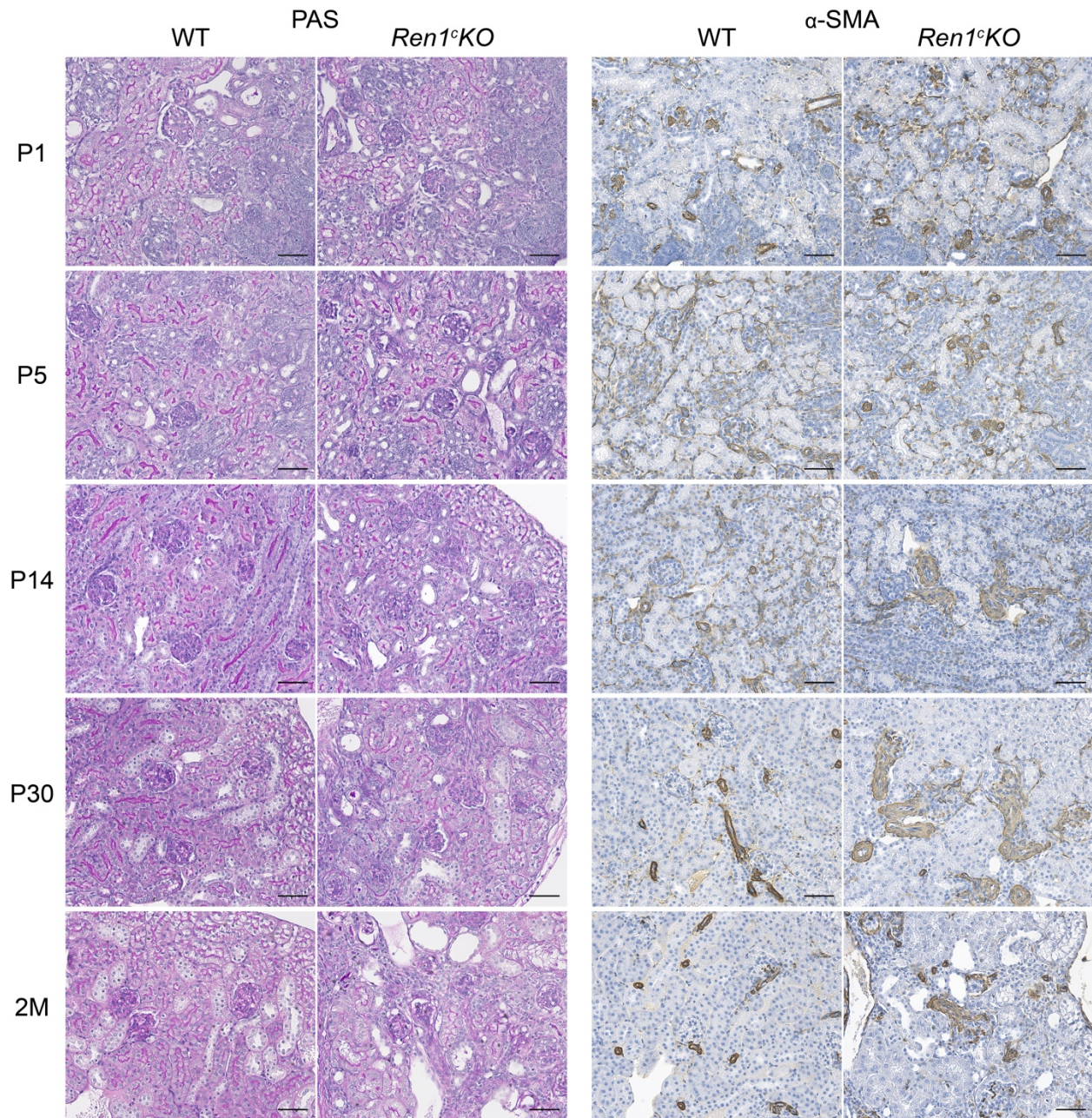


**Supplemental Figure 3. Vascular abnormality in *Ren1$^c$KO* mice at different time points**. PAS staining and immunohistochemistry for α-SMA in *Ren1$^c$KO* mouse kidneys and their controls at P1, P5, P14, P30, and 2 months of age. The afferent arteriolar hypertrophy was significantly detected in *Ren1$^c$KO* mice starting at P14. Scale bars, 50 μm. α-SMA; α-smooth muscle actin, *Ren1$^c$KO*; *Ren1$^c$* gene knockout, WT; wild-type.

## Supplemental Figure 4
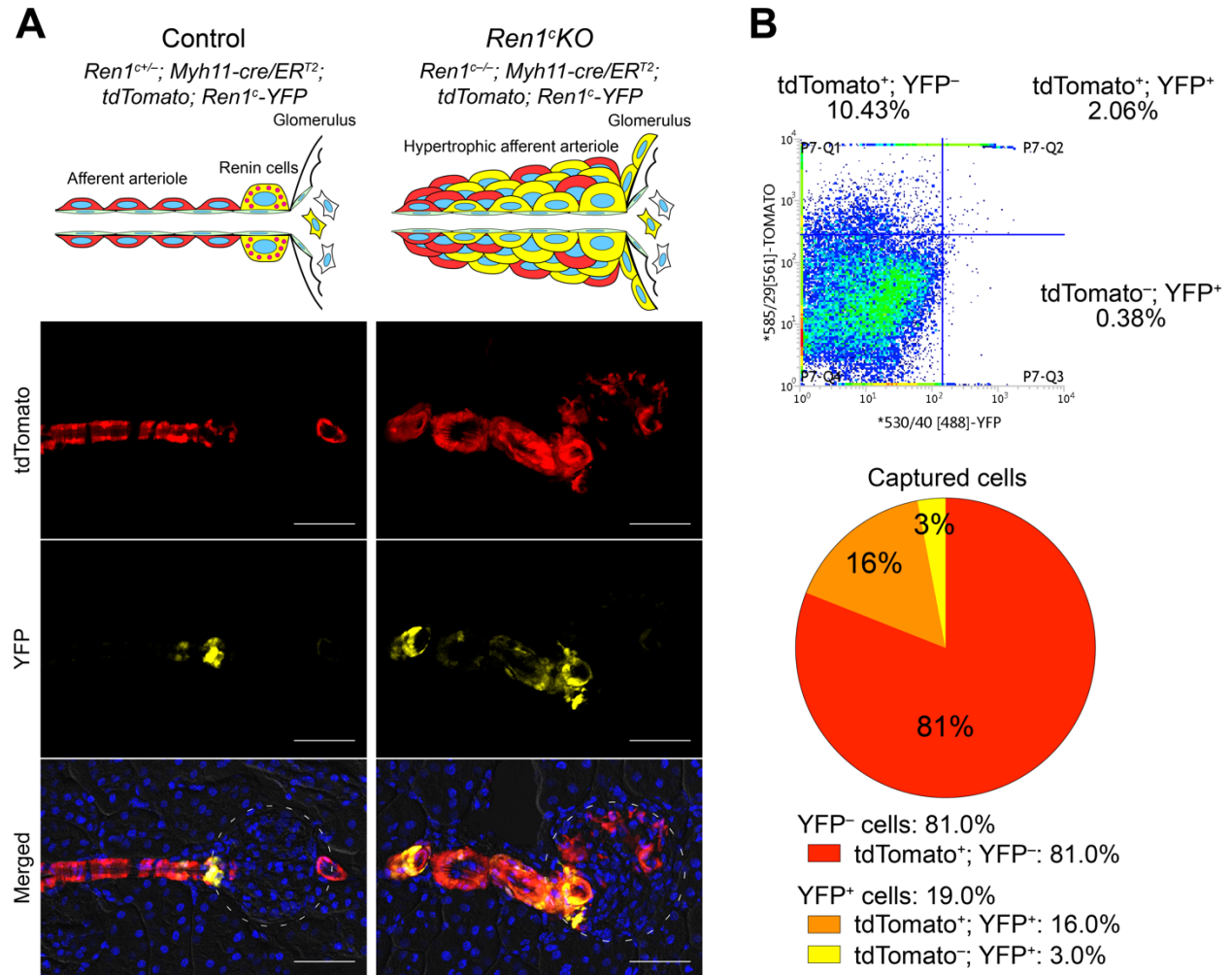


**Supplemental Figure 4. Labeling *Renin$^{null}$* cells and other vascular SMCs.** (**A**) Kidney sections from *Ren1$^{c+/-}$;Myh11-CreER$^{T2}$;tdTomato;Ren1$^c$-YFP* mouse and *Ren1$^{c-/-}$;Myh11-CreER$^{T2}$;tdTomato;Ren1$^c$-YFP* mouse. Vascular SMCs were labeled with tdTomato, and WT renin cells and *Renin$^{null}$* cells were labeled with YFP. The merged pictures also show nuclear staining by Hoechst and differential interference contrast microscopy. Scale bars, 50 µm. (**B**) FACS results of *Ren1$^{c-/-}$;Myh11-CreER$^{T2}$;tdTomato;Ren1$^c$-YFP* mouse kidney. Of the isolated cells, 19% were the *Renin$^{null}$* cells (16.0% and 3.0% were tdTomato$^+$;YFP$^+$ and were tdTomato$^-$;YFP$^+$, respectively), and 81.0% were other tdTomato$^+$;YFP$^-$ vascular SMCs. FACS; fluorescence-activated cell sorting, *Ren1$^c$KO*; *Ren1$^c$* gene knockout, SMCs; smooth muscle cells.

**Supplemental Figure 5**
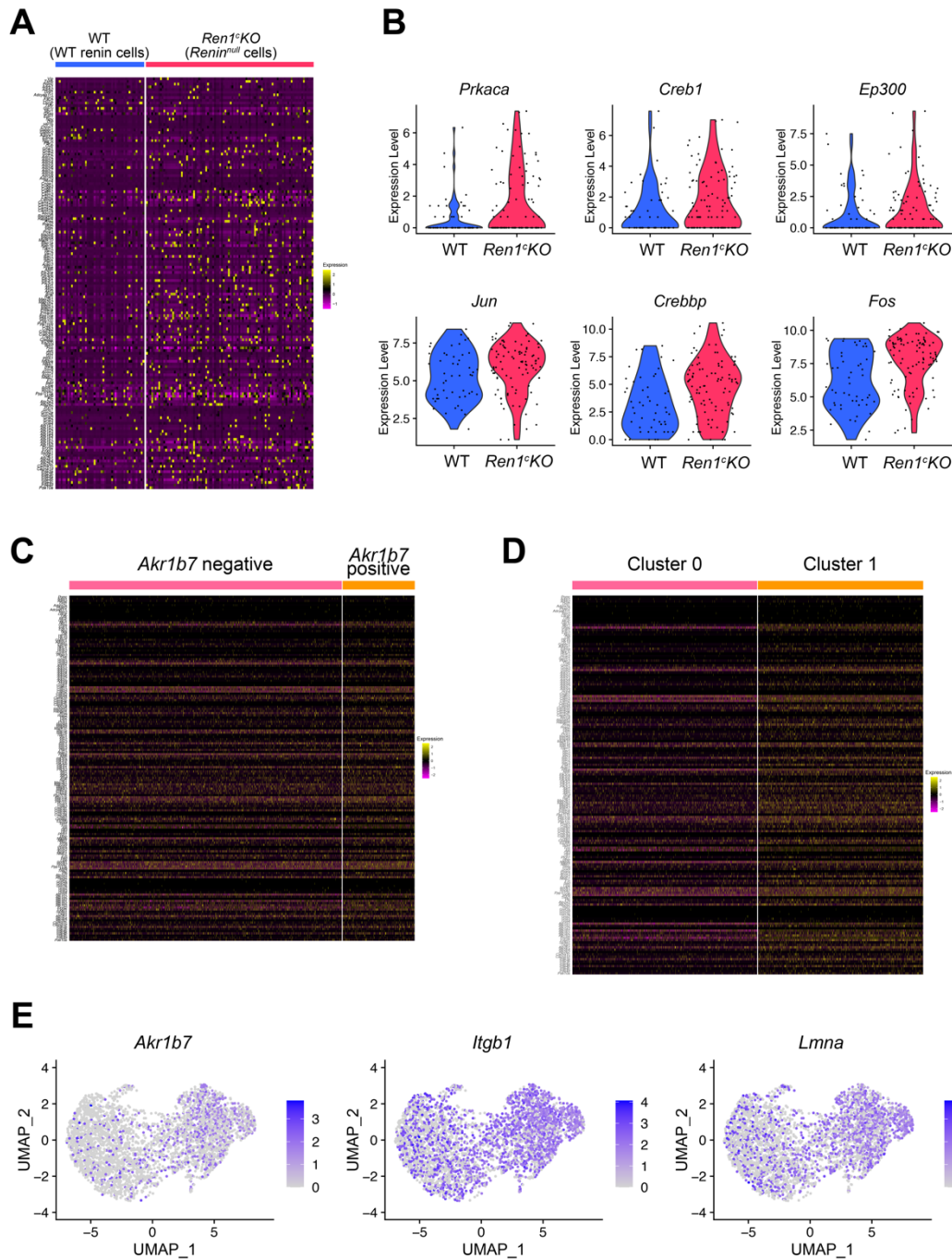


**Supplemental Figure 5. scRNA-seq of cAMP pathway and mechanotransduction related genes.** (**A**) Heatmap of the cAMP pathway genes from scRNA-seq of WT renin cells and *Renin^null* cells (C1 system). (**B**) Violin plots of the major cAMP pathway-related genes by C1 scRNAseq. (**C, D**) Heatmap of the cAMP pathway genes from scRNA-seq of *Ren1^cKO;SMMHC-CreER^T2;tdTomato;Ren1^c-YFP* mice (Chromium System). (**E**) Feature plots of UMAP for *Akr1b7, Itgb1,* and *Lmna* in scRNA-seq of Chromium System. *Ren1^cKO*; *Ren1^c* gene knockout, scRNA-seq; single-cell-RNA sequencing, UMAP; Uniform Manifold Approximation and Projection, WT; wild-type.

**Supplemental Figure 6**
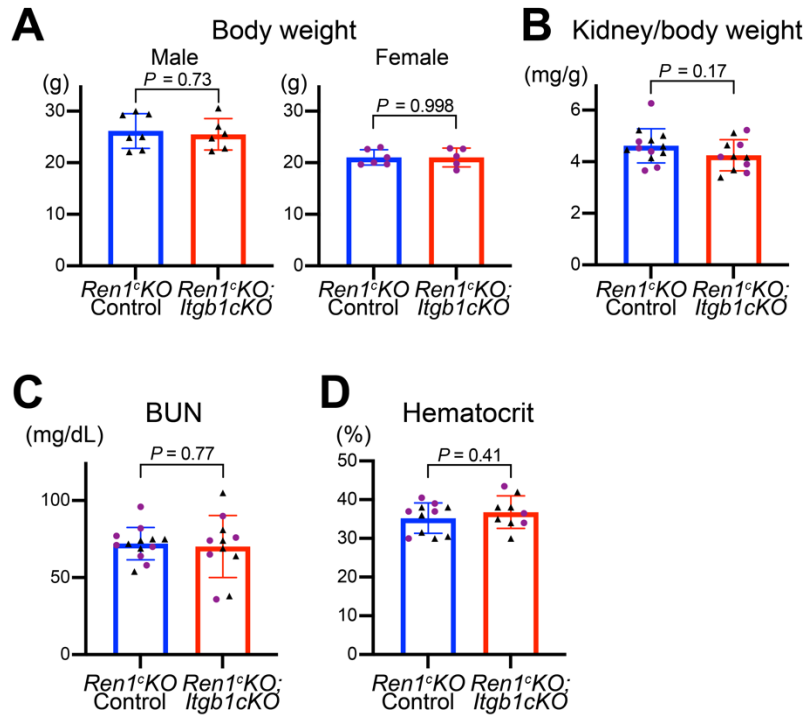


**Supplemental Figure 6. The phenotype of the *Ren1<sup>c</sup>KO;Itgb1cKO* mouse.** (**A, B**) Body sizes were not different between *Ren1<sup>c</sup>KO* control and *Ren1<sup>c</sup>KO;Itgb1cKO* mice. There was no significant difference in body weight (**A**; male $n{\geq}6$, female $n{\geq}5$) and kidney/body weight rate (**B**; $n{\geq}11$) (Student's t-test). (**C, D**) Blood tests did not differ in *Ren1<sup>c</sup>KO* control and *Ren1<sup>c</sup>KO;Itgb1cKO* mice. There was no significant difference in BUN (**C**; $n{\geq}11$) and hematocrit (**D**; $n{\geq}9$) (Student's t-test). All data are reported as means ± standard deviation. Black triangles show male samples, and purple dots show female samples. BUN; blood urea nitrogen, *Itgb1cKO*; deletion of the *Itgb1* gene in cells of the renin lineage, *Ren1<sup>c</sup>KO*; *Ren1<sup>c</sup>* gene knockout.

**Supplemental Figure 7**
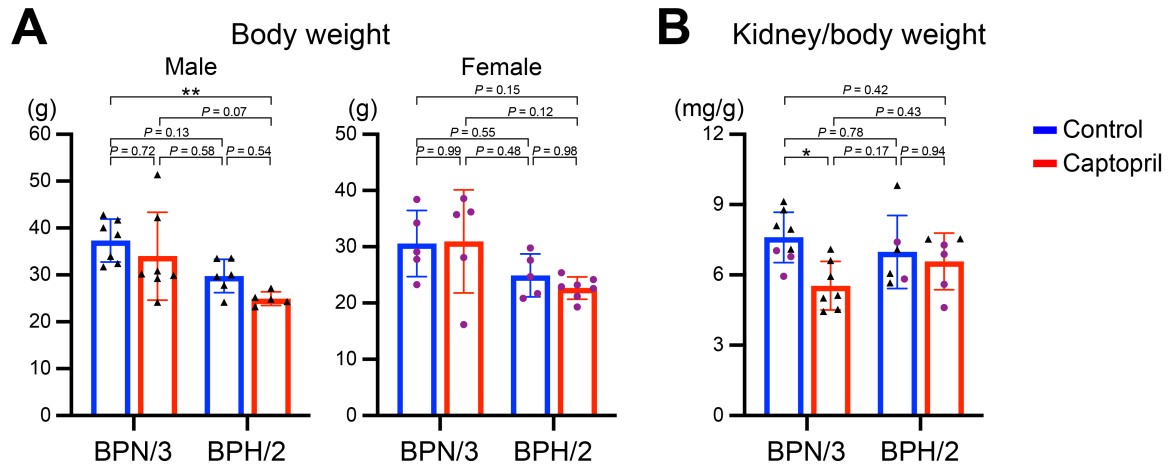


**Supplemental Figure 7. Phenotypes of the BPN/3 and BPH/2 mice with and without long-term inhibition of RAS.** (**A**) Body sizes were not different between with and without long-term usage of captopril in both BPN/3 and BPH/2 mice (*n*≥5, two-way ANOVA followed by Tukey's multiple comparison test). (**B**) Kidney/body weight rates were decreased by long-term usage of captopril in BPN/3 mice, but not in BPH/2 mice *(n*≥6, two-way ANOVA followed by Tukey's multiple comparison test). All data are reported as means ± standard deviation. Black triangles show male samples, and purple dots show female samples. *$P$<0.05, **$P$<0.01.

## Supplemental Figure 8
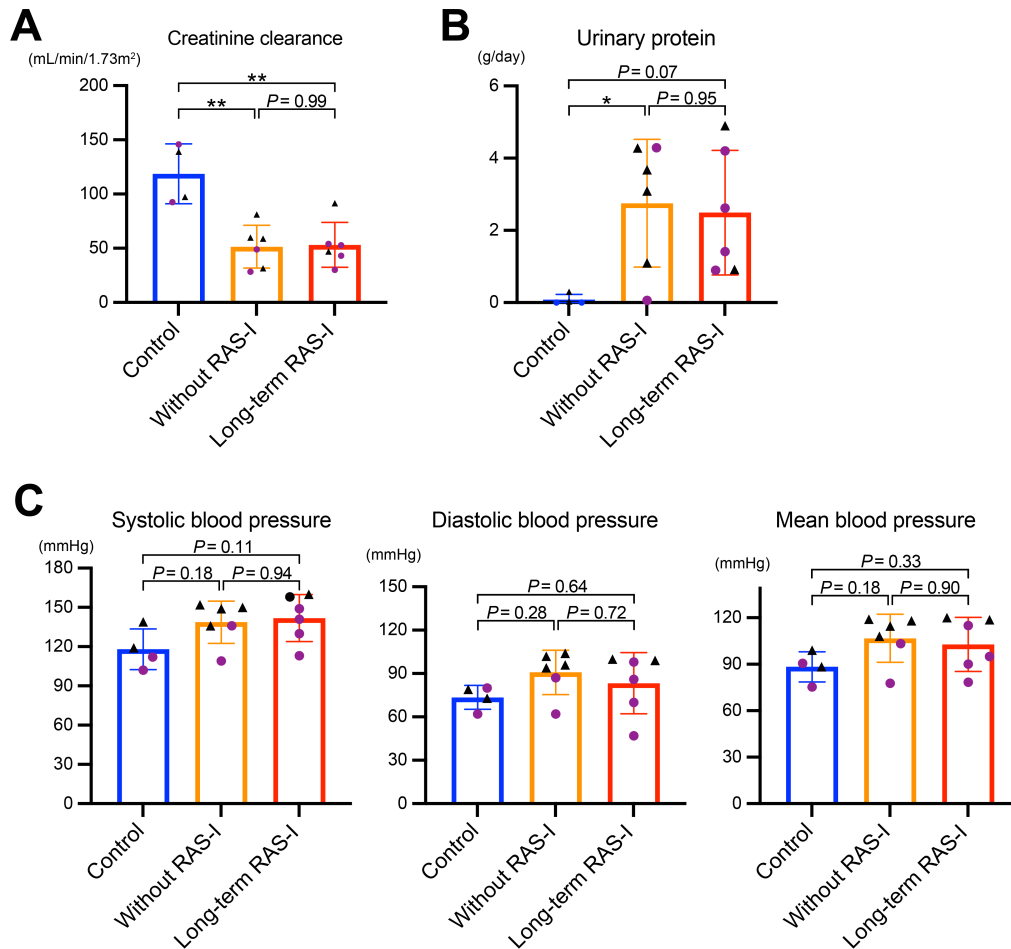


**Supplemental Figure 8. The background of the human samples.** (**A**) The creatinine clearance of patients with long-term usage of RASi (*n*=6) was not significantly different from patients with nephrosclerosis without RASi (*n*=6) (One-way ANOVA followed by Tukey's multiple comparisons test). (**B**) The urinary protein of patients with long-term usage of RASi (*n*=6) was not significantly different from patients with nephrosclerosis without RASi (*n*=6) (One-way ANOVA followed by Tukey's multiple comparisons test). (**C**) Blood pressure was not different between patients with long-term usage of RASi (*n*=6), healthy controls (*n*=4), and patients with nephrosclerosis without RASi (*n*=6) (One-way ANOVA followed by Tukey's multiple comparisons test). All data are reported as means ± standard deviation. Black triangles show male samples, and purple dots show female samples. *$P<0.05$, **$P<0.01$. RASi; renin-angiotensin system inhibitor.